Received: 16 January 2019 | Revised: 22 March 2019 | Accepted: 24 March 2019

DOI: 10.1002/jbio.201900019

FULL ARTICLE

JOURNAL OF BIOPHOTONICS

Refractive index measurement using single fiber reflectance spectroscopy

Xu U. Zhang[1]* | Dirk J. Faber[1] | Anouk L. Post[1,2] | Ton G. van Leeuwen[1] | Henricus J. C. M. Sterenborg[1,2]

[1]Biomedical Engineering and Physics, Amsterdam UMC, University of Amsterdam, Amsterdam, The Netherlands

[2]Department of Surgery, The Netherlands Cancer Institute, Amsterdam, The Netherlands

***Correspondence**
Xu U. Zhang, Biomedical Engineering and Physics, Amsterdam UMC, University of Amsterdam, Meibergdreef 9, Amsterdam 1105 AZ, The Netherlands.
Email: xu.zhang@amc.uva.nl

Funding information
NWO-TTW, Grant/Award Number: 12702; Netherlands Organization for Scientific Research, Grant/Award Number: 12702

A method using single fiber reflectance spectroscopy to measure the refractive indices of transparent and turbid media over a broad wavelength range is presented and tested. For transparent liquid samples, the accuracy is within 0.2%, and the accuracy increases with increasing wavelength. For liquid turbid media, the accuracy is within 0.3% and increases with decreasing wavelength. For solid turbid samples, such as human skin, the accuracy critically depends on the optical contact between the fiber and sample surface. It is demonstrated that this technique has the potential to measure refractive indices of biological tissue in vivo.

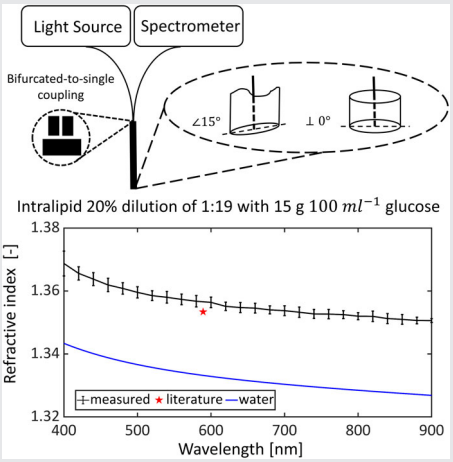

KEYWORDS
Fresnel reflection, refractive index, single fiber reflectance, transparent, turbid

1 | INTRODUCTION

The refractive index is of great importance for applications in both engineering and research. Spatial variation of the refractive index causes light scattering; therefore, it is an indispensable input for modeling light propagation in turbid media [1, 2]. The refractive index itself depends on the local molecular density and thus carries information on, for example, the microstructure of biological tissues [3]. In addition, the measurement of the refractive index can be used in various applications such as the monitoring of the concentration of solutes in fluids [4–6].

Commercial and modified Abbe refractometers are common instruments to measure the refractive indices of both transparent and turbid media [7, 8]. For optimal accuracy, these instruments usually have a narrow band light source to avoid dispersion by the instrument components. Consequently, only the refractive index at a single wavelength is obtained (eg, at the Sodium D-line of 589 nm). Furthermore, conventional Abbe refractometers are usually limited to the visible wavelength range. To extend the detection spectral range to the near infrared/infrared, a suitable detector needs to be integrated [9]. Methods based on optical coherence tomography (OCT) have been developed to measure refractive indices of both in vitro and in vivo human tissue. Refractive index measurements with OCT usually require alignment of optical elements, which is the main factor limiting the accuracy. [10–12] Extensions of OCT using

differential phase contrast can improve the accuracy by an order of magnitude. However, OCT systems are relatively costly. Chang et al developed a fiber optic Fresnel ratio meter to measure the refractive indices of transparent media with a simple and low budget method with a precision of 2.5×10^{-5}. [13] However, this method is not applicable to turbid media, and because a laser diode is used as the light source, only the refractive index value at a single wavelength is obtained. Moreover, this method requires the knowledge of the effective refractive index of the optical fibers used. The accuracy of this input will directly influence the accuracy of the measurement result.

In this study, we present a method based on single fiber reflectance (SFR) spectroscopy to measure the refractive indices (phase index) of both transparent and turbid media over a broad wavelength range. [14] The measurement on transparent media is based on the Fresnel reflection from a flat polished fiber tip, caused by the refractive index mismatch between the fiber and the sample in contact. The measurement on turbid media requires two fibers: one flat polished fiber that collects both the back-scattering signal from the turbid sample and the Fresnel reflection signal at the fiber tip, and the other fiber polished at a certain angle that collects only the back-scattering signal. This method does not require optical alignment, but only the well-established refractive indices of air and water. It allows us to obtain a broad wavelength refractive index spectrum instead of a refractive index value at a certain single wavelength. The refractive indices of various transparent and turbid samples are measured with this technique and compared with the values from the literature. Finally, we provide a preliminary in vivo demonstration on a volunteer's skin.

2 | METHODOLOGY

2.1 | Setup

The schematic diagram of an SFR setup is illustrated in Figure 1. White light was emitted by a halogen light source (Ocean Optics, HL-2000, broadband unpolarized light) and coupled through one branch of a bifurcated fiber into a multimode measurement fiber optic probe that is in contact with the sample. The light was reflected back and guided back through the other branch of the bifurcated fiber into the spectrometer (Avantes, Avaspec-ULS2048L Starline). For transparent media, a single flat polished fiber optic probe with SMA connectors at both ends was used; for turbid media, additional to the flat polished fiber optic probe, a fiber with the measurement end polished at 15° was used. The angle-polished probe had an SMA connector on the side connected to the bifurcated fiber, while the measurement end of the fiber was glued into the center of a 5 mm diameter

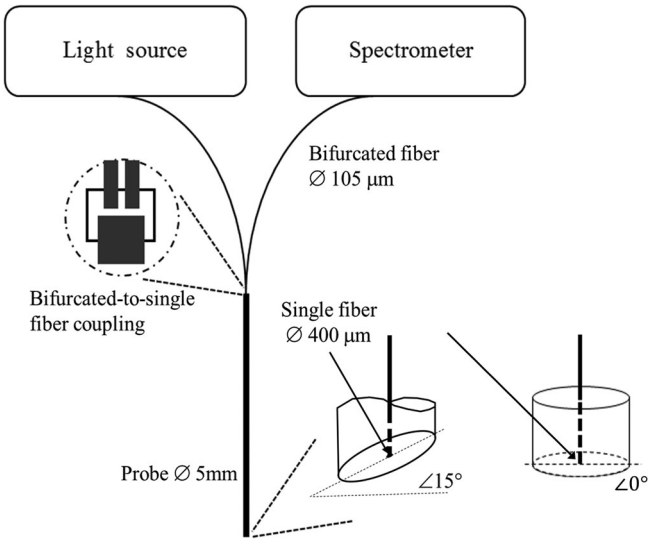

FIGURE 1 Schematic of single fiber reflectance spectroscopy with a flat and angle polished (15°) fiber probe

aluminum tubing. The tubing surface was also polished at a 15° angle and aligned with the fiber surface. Both probes were made of a 400 µm diameter multimode fiber from the same batch. The NA of the fiber is 0.22 ± 0.02 according to the fiber supplier. [15] The measurement system was kept static during all measurements to ensure a stationary coupling efficiency between optical components. The 2-m measurement fiber was bended by 90° to reduce the cladding modes. Besides, the bifurcated-single coupling and the NA of the spectrometer also exclude the cladding modes inherently.

2.2 | Measurement of the refractive index using SFR

The refractive index measurement using SFR is based on a simplified Fresnel reflection at the flat polished fiber tip due to the refractive index mismatch between the fiber and the sample in contact. The simplification assumes that the Fresnel reflection is insensitive to the incident angle when the incident angular range is small, homogeneous semi-infinite samples and perfect contact between the fiber and sample. For a given sample, the Fresnel reflection can then be expressed by Equation (1).

$$R = \frac{(n_f - n_s)^2}{(n_f + n_s)^2}. \quad (1)$$

This equation can be solved for the refractive index of the sample, provided R can be determined and the effective index of the fiber, n_f, is known, as shown in Equation (2).

$$n_s = n_f \times \frac{1-\sqrt{R}}{1+\sqrt{R}}. \quad (2)$$

As described by Zhang et al [16], n_f can be determined from the measured reflected intensity spectra of two compounds with well-known refractive indices, that is, water and air.

2.2.1 | Measurement of the refractive indices of transparent media

For this measurement, the fiber tip was slightly immersed. The process of determining the refractive index of a transparent sample using SFR is shown in the flowchart in Figure 2. First, the Fresnel reflection at the fiber-sample surface R is obtained by measuring the reflected intensity spectra of the sample I_s and of a compound with a well-known refractive index, that is, air I_{air}, using a flat polished fiber Equation (3):

$$R = R_{\text{air}} \times \frac{I_s - I_d}{I_{\text{air}} - I_d}. \quad (3)$$

I_d is subtracted from I_s and I_{air} to account for the dark current of the spectrometer and ambient light, measured by blocking the light source. R_{air} was calculated using the Fresnel equation with the effective index of the fiber, n_f, and air, n_{air}, (equal to 1). n_f was determined from measured reflected intensity spectra of water I_{water} and air I_{air}. [16] Combining Equations (2) and (3), n_s was solved numerically. Note that two solutions of n_s were found symmetrically around n_f. Only the lower value was deemed realistic for our samples which all had $n_f > n_s$.

2.2.2 | Measurement of the refractive indices of turbid media

For turbid samples, the assumption of perfect contact and the homogeneous semi-infinite samples may not be satisfied. The retrieved refractive index should therefore be regarded as pseudo-index of refraction. However, for turbid samples, there is also a contribution of back-scattered light to the measured reflectance. To correct for this contribution, besides SFR measurements performed on the sample with a flat polished fiber, additional SFR measurements were performed on the same sample with an angle polished fiber. The angle polished fiber was made from the same batch of fiber (NA 0.22) and polished at 15° to eliminate the Fresnel reflection between fiber and sample. Thus, the reflectance measured by the flat polished fiber, $R_\perp$, has contributions from the Fresnel reflection, as well as the back-scattering from the sample. Contrariwise, for the angle-polished fiber, it is assumed that the Fresnel reflection is completely eliminated, so the reflectance measured by the angle polished fiber, $R_\angle$, is used to estimate the contribution of the back-scattering from the sample. By further assuming that the flat and angle polished probes have an identical collection efficiency of the back scattered light, the Fresnel reflection is given by $R = R_\perp - R_\angle$, from which the refractive index of the sample in contact can be determined using Equation (2).

To determine R, a turbid sample with known absolute reflectance, that is, undiluted Intralipid-20%, is required as an intermediate reference to correlate the reflected intensity measured by the flat and angle polished fibers.

The process of determining the refractive index of a turbid sample using SFR is shown in the flowchart in Figure 3. We first performed SFR measurements of air, $I_{\perp,\ \text{air}}$, water, $I_{\perp,\ \text{water}}$, undiluted Intralipid-20% $I_{\perp,\ IL}$, and the turbid sample, $I_{\perp,\ s}$ by immersing the flat polished fiber in the respective measurement samples. The dark current, $I_{\perp,\ d}$, the Fresnel reflection at the fiber-air interface R_{air} and the effective index of the fiber, n_f, were determined as above. The absolute reflectance of undiluted Intralipid-20% by the SFR setup could be obtained using Equation (4):

$$R_{IL} = R_{\text{air}} \times \frac{I_{\perp,\text{IL}} - I_{\perp,\text{water}}}{I_{\perp,\text{air}} - I_{\perp,\text{d}}}. \quad (4)$$

$I_{\perp,\ \text{water}}$ was subtracted from $I_{\perp,\ IL}$ to account for the internal reflection due to the refractive index mismatch at the fiber tip, the ambient light and the dark current of the spectrometer, so that only the contribution of the back-scattering light remained. $I_{\perp,\ d}$ was subtracted from $I_{\perp,\ \text{air}}$ to account for the ambient light and the dark current of the spectrometer. The sum of the measured absolute reflectance of the back-scattered light from the turbid sample and the Fresnel reflection at the fiber tip was calculated using Equation (5).

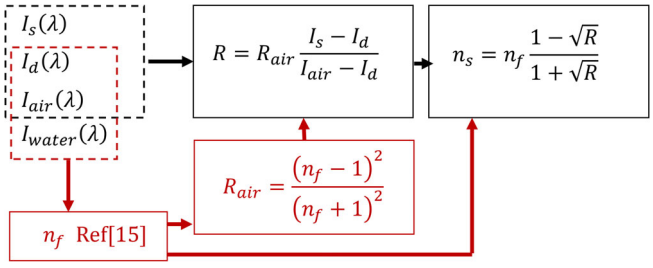

FIGURE 2 Flowchart to determine the refractive index of a transparent sample. $I_x(\lambda)$ are raw spectra [counts] resulting from the reflected intensities of (m)edium, air and water, respectively; and (d)ark current. The red part of the flow chart concerns det ermination of the effective index of the fiber n_f and corresponding Fresnel reflection at the fiber-air interface R_{air}

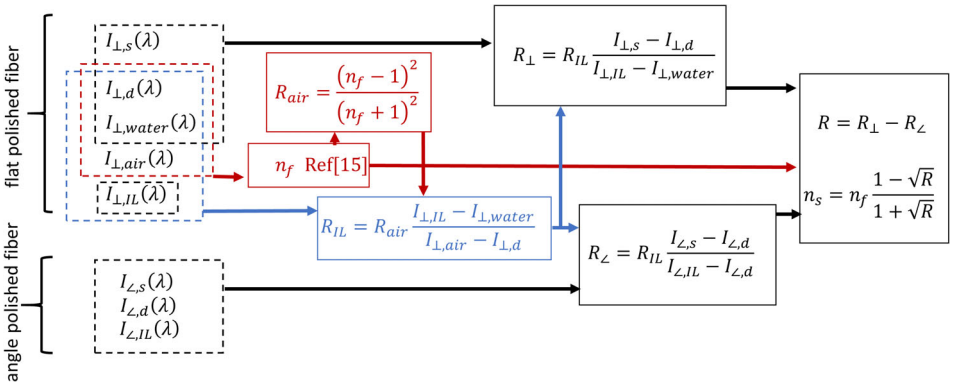

FIGURE 3 Flowchart to determine the refractive index of a turbid sample. $I_{\perp,x}(\lambda)$ and $I_{\angle,x}(\lambda)$ are raw spectra [counts] resulting from the reflected intensities of respective measurement objects and (d)ark current. The red part of the flow chart concerns the determination of the effective index of the fiber n_f and the corresponding Fresnel reflection at the flat polished fiber-air interface R_{air}; the blue part of the flow chart concerns the determination of the measured absolute reflectance of undiluted Intralipid-20% R_{IL} and the intermediate correlation between the sample spectra measured by the flat $R_\perp$ and angle polished fiber $R_\angle$

$$R_\perp = R_{IL} \times \frac{I_{\perp,\mathrm{s}} - I_{\perp,\mathrm{d}}}{I_{\perp,\mathrm{IL}} - I_{\perp,\mathrm{water}}}. \quad (5)$$

SFR measurements were then performed on the same undiluted Intralipid-20% sample, $I_{\angle,IL}$, and turbid sample, $I_{\angle,s}$, by immersing the angle-polished probe in the respective measurement samples. The measured absolute reflectance of the back-scattering light from the turbid medium was calculated using Equation (6).

$$R_\angle = R_{IL} \times \frac{I_{\angle,\mathrm{s}} - I_{\angle,\mathrm{d}}}{I_{\angle,\mathrm{IL}} - I_{\angle,\mathrm{d}}}. \quad (6)$$

R was calculated by subtracting $R_\angle$ from $R_\perp$, with which the pseudo-index of refraction of the turbid sample was calculated using Equation (2). We will refer to the pseudo-index of refraction as the refractive index of the turbid medium from here.

2.3 | Sample preparation

We applied this method to transparent samples: ethanol and D-glucose aqueous solutions of three different concentrations: 5 g 100 mL^{-1}, 10 g 100 mL^{-1} and 15 g 100 mL^{-1}. We also measured the refractive indices of turbid samples: Intralipid-20% dilutions of 1:4, 1:9, 1:19 and 1:39. Each Intralipid-20% dilution of 1:X was made by mixing one portion of undiluted Intralipid-20% with X portions of demineralized water. Another turbid sample was also made by mixing Intralipid-20% dilution of 1:19 with dissolved D-glucose powder so the glucose concentration of the solution was 15 g 100 mL^{-1}. Intralipid-20% samples were made and shaken before the measurements so the lipid particles were homogenously distributed in the container.

A preliminary demonstration was also performed in vivo on the inner forearm skin and the callus on the palm of a volunteer. Demineralized water was applied between the probe and measurement spot to improve the optical contact. The pressure was applied by pushing the probe onto the measurement spot to maximize the contact between the probe and skin.

2.4 | Data analysis

Five sets of measurements on the transparent samples were performed following the procedure explained in the flowcharts in Figures 2 and 3. For measurements on turbid samples, each set of the measurements with the flat polished fiber generated one spectrum of n_{eff}, R_{IL} and $R_\perp$ while each set of the measurements with the angle polished fiber generated one spectrum of $R_\angle$. Each combination of n_{eff}, R_{IL}, $R_\perp$ and $R_\angle$ yielded one refractive index spectrum of the sample in contact n_s. The measurements with the flat and angle polished fibers were performed five times each, thus there were 25 combinations. The average and SD of the refractive indices of all measured samples at each wavelength were calculated from 400 to 900 nm.

3 | RESULTS

The average and SD of the refractive index of ethanol were calculated and are plotted together with the refractive index of ethanol as obtained from literature in Figure 4. [17] The error bar plotted is one SD. The measured refractive index of ethanol is lower than the refractive index from literature. The difference is roughly 0.2% and decreases as the wavelength increases. The difference at 900 nm is roughly 0.01%. The relative error (ratio of one SD over the average

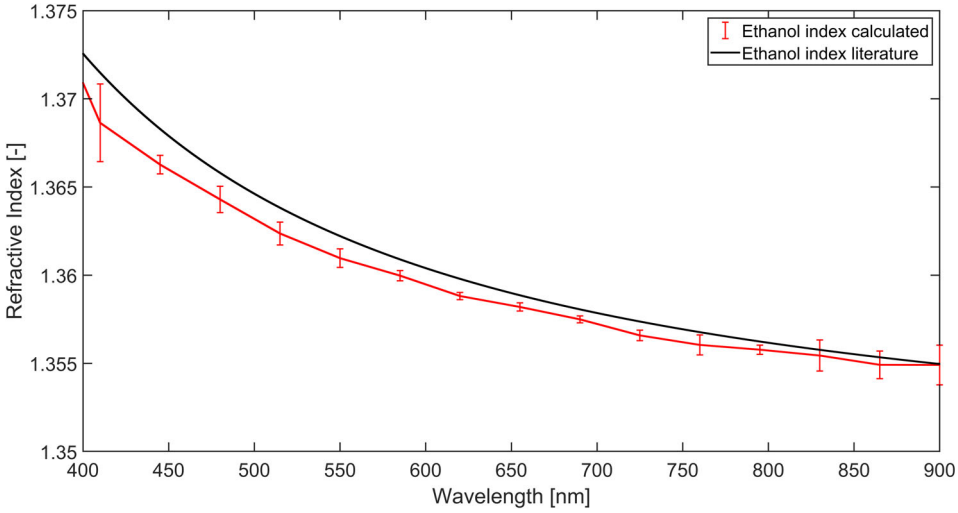

FIGURE 4 The measured refractive index of ethanol (Red line) and the refractive index of ethanol from literature [17] (black line)

[SD/mean]) is below 4×10^{-4} for most wavelengths and is relatively larger in the beginning (400-450 nm) and the end (850-900 nm) of the measured wavelength range.

The average and SD of the measured refractive indices of glucose solutions were calculated and are plotted together with the refractive indices of the glucose solutions of the same concentrations as obtained from the literature at 589.2 nm in Figure 5. [18] The error bar plotted is one SD. The difference between the average of the measured refractive indices and the values from the literature is −0.03%, +0.02% and + 0.06% for concentrations of 5,10 and 15 g 100 mL^{-1} respectively. The SD/mean value increases with increasing glucose concentration while for each solution, it decreases with increasing wavelength. For the glucose concentration of 5 g 100 mL^{-1}, the SD/mean values roughly decrease from 1.2×10^{-3} at 400 nm to 0.4×10^{-3} at 900 nm; for the glucose concentration of 10 g 100 mL^{-1}, from 2.5×10^{-3} at 400 nm to 0.7×10^{-3} at 900 nm; for the glucose concentration of 15 g 100 mL^{-1}, from 3×10^{-3} at 400 nm to 1.2×10^{-3} at 900 nm.

The average and SD of refractive indices of undiluted Intralipid-20% and Intralipid-20% dilutions of 1:4, 1:9, 1:19 and 1:39 were calculated and are plotted together with the refractive index of water, [19] which is the solvent in all Intralipid-20% samples (Figure 6). The error bar plotted is one SD. The average of the measured refractive index of the undiluted Intralipid-20% has the best match with the refractive index of water from literature compared with the measured refractive indices of Intralipid-20% dilutions. For undiluted Intralipid-20%, the difference between measured values and literature is below 0.02%. For Intralipid-20% dilutions, the difference between the measured refractive indices and the refractive index of water is roughly within 0.3%. It is wavelength dependent and increases as the wavelength increases.

The average and SD of the refractive index of Intralipid-20% dilution of 1:19 with a glucose concentration of 15 g 100 mL^{-1} were calculated and are plotted in Figure 7 together with the refractive index of glucose solution of 15 g 100 mL^{-1} at 589.2 nm from literature. [18] The error bar

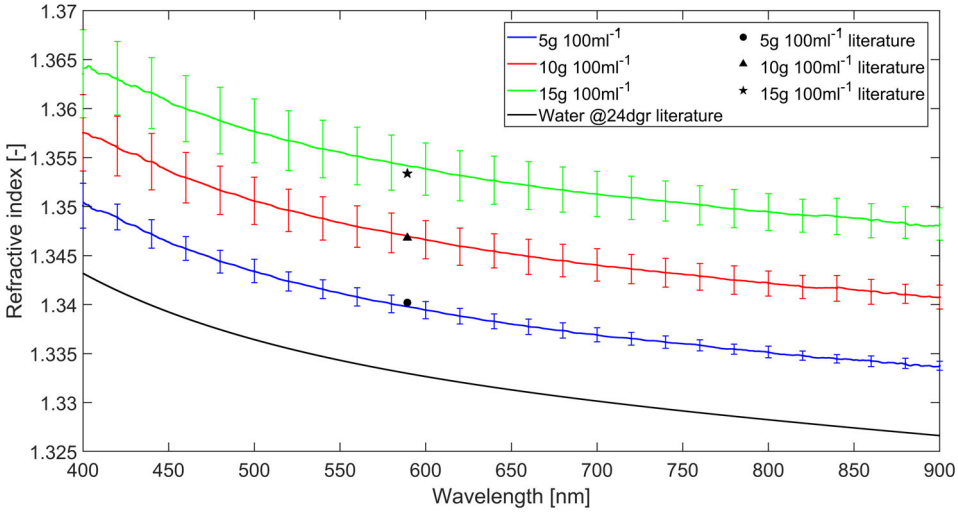

FIGURE 5 Calculated refractive indices of D-glucose solutions (blue line: 5 g 100 mL^{-1}; red line: 10 g 100 mL^{-1}; green line: 15 g 100 mL^{-1}), the refractive indices of the D-glucose solutions of the same concentrations from literature [18] (black dot: 5 g 100 mL^{-1}; black triangle: 10 g 100 mL^{-1}; black star: 15 g 100 mL^{-1}) and the refractive index of water from literature [19] (black line)

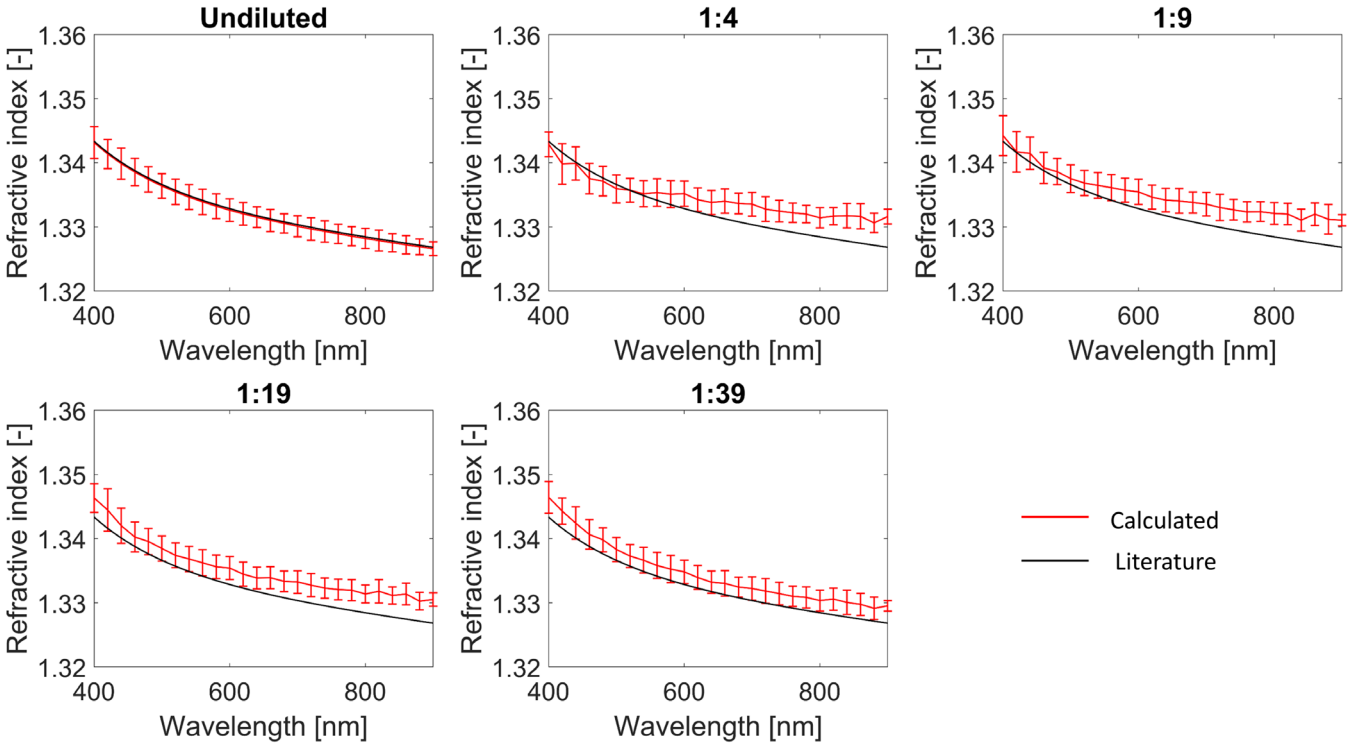

FIGURE 6 Calculated refractive indices of undiluted Intralipid-20%, Intralipid-20% dilutions of 1:4, 1:9, 1:19, 1:39 and the refractive index of water from literature [19]

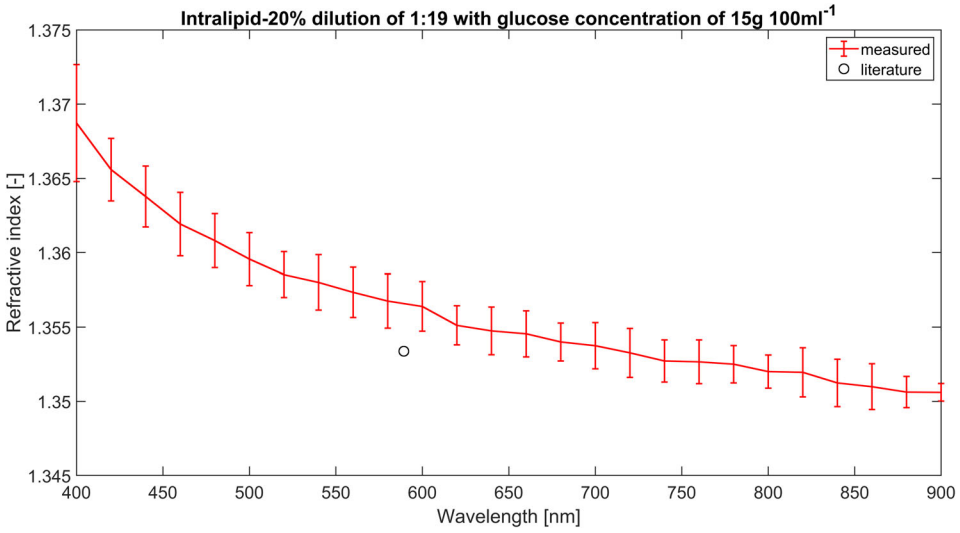

FIGURE 7 The calculated refractive index of Intralipid-20% dilution of 1:19 with D-glucose concentration of 15 g 100 mL^{-1} and the refractive index of the D-glucose solution of 15 g 100 mL^{-1} from literature [18]

plotted is one SD. The average of the measured refractive index at 589 nm is 0.23% higher than the value from the literature. The SD/mean decreases with increasing wavelength from roughly 2.5 $\times 10^{-3}$ at 400 nm to below 1×10^{-3} at 900 nm.

The calculated refractive indices of the inner forearm skin and the callus on the palm of one volunteer were calculated and are plotted in Figure 8. The refractive index of the inner forearm skin is lower than the refractive index of the callus of the volunteer. The values range roughly from 1.37 to 1.41.

4 | DISCUSSION

We present a method based on SFR to measure the refractive index of both transparent and turbid media. The measurement on transparent media is based on the Fresnel reflection from a flat polished fiber tip. The measurement on turbid media used one flat polished fiber that collects both the back-scattering signal from the turbid sample and the Fresnel reflection signal at the fiber tip, and the other fiber polished at a certain angle that collects only the back-scattering signal. This method does not require optical alignment, but

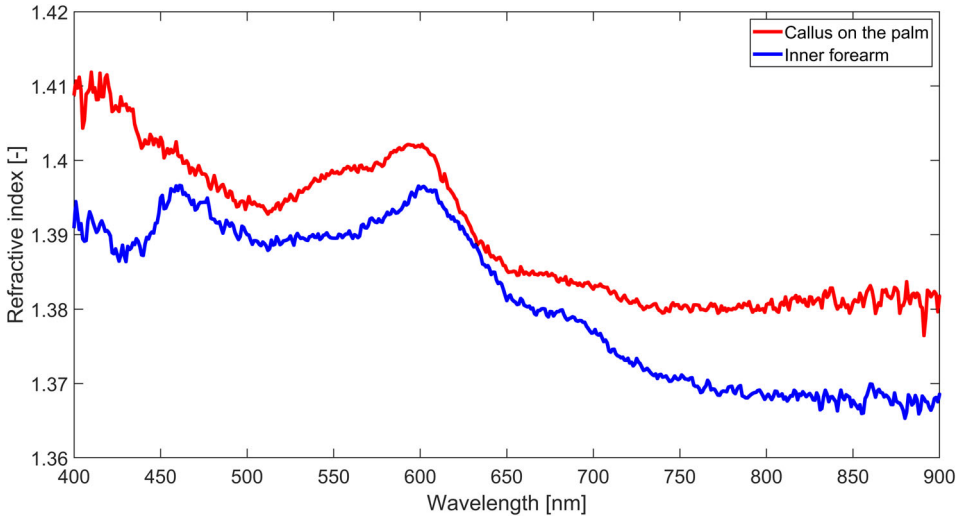

FIGURE 8 Measured refractive indices of callus on the palm (red) of the volunteer and the inner forearm skin (blue)

only the well-established refractive indices of air and water. It allows us to obtain a refractive index spectrum instead of a refractive index value at a certain single wavelength. The method was tested on various transparent and turbid samples. The results were compared with values from the literature and accuracy within 0.2% and 0.3% was achieved for the transparent and turbid samples respectively.

4.1 | Measurements on transparent media

The measured refractive indices of ethanol and glucose solutions accurately match the refractive indices measured previously. The difference between the average of the measured refractive indices and the refractive indices from the literature decrease as the wavelength increases. This wavelength dependency could be attributed to the relatively low reflected intensity in the lower wavelength range. The accuracy of measurements on the glucose solution of 5 g 100 mL^{-1} and 10 g 100 mL^{-1} is higher than the glucose solution of 15 g 100 mL^{-1}, which can be explained by the decrease of the signal-to-noise ratio as the concentration increases. The higher the concentration is, the better the refractive index match is between the fiber and the sample, the lower the reflected intensity becomes. The difference between the measured values and values from the literature indicates the accuracy of the method while the SD/mean values indicate the precision of the method. The precision is not as good as the accuracy of this method, which suggests that multiple measurements should be performed and the results should be averaged when measuring the refractive index with SFR.

4.2 | Measurements on turbid media

For turbid samples, the assumption of perfect contact and the homogeneous semi-infinite samples used to derive Equation (1) may not be satisfied. The retrieved refractive index should therefore be regarded as pseudo-index of refraction. The measured refractive indices of all Intralipid-20% samples deviated slightly (within 0.3%) from the refractive index of water, which was the solvent of undiluted Intralipid-20% and Intralipid-20% dilutions. The small magnitude of the deviation indicated that the lipid particles were barely in contact with the fiber surface. Because the concentration of scatterers in all the measured aqueous samples is relatively low, it was expected that no lipid particles were in contact with the fiber surface. Thus, we can conclude that when applying our method on liquid turbid media of relatively low scatterer concentration, the refractive index of the solvent is measured. In the situation of high scatterer concentration, the number of scatterers that are in contact with the fiber surface might also increase, so that when applying our method, the retrieved pseudo-index of refraction has the contribution from both the solvent and the scatterers. The average refractive index of undiluted Intralipid-20% has the best match with the refractive index of water. This match can be explained by the fact that the same undiluted Intralipid-20% was used as the sample and reference at the same time. Thus, $R_{\angle}$ always equaled R_{IL}, which was determined by the measurements with the flat polished fiber. As a result, R equals to $R_{\mathrm{IL}} \times \frac{I_{\perp,\mathrm{water}} - I_{\perp,\mathrm{d}}}{I_{\perp,\mathrm{IL}} - I_{\perp,\mathrm{water}}}$, which only depends on the measurements using the flat-polished probe; the bias caused by the possible difference in the collection efficiency of the flat and angle-polished probes was eliminated. However, for Intralipid-20% dilutions, the sample is different from the reference. If the angle-polished probe had a different collection efficiency compared with the flat-polished probe, the different collection efficiency would have an influence on the results.

Given what has been discussed above, there might be two explanations that limit the accuracy of this technique to measure the refractive index of turbid media. One is a

residual internal reflection from the angle-polished probe. We assume the internal reflection was completely eliminated when our fiber optic probe with NA 0.22 is polished at 15 degrees. However, experiments showed that the internal reflection was found to be significantly reduced but not completely eliminated. This residual reflectance may be related to the polishing quality. For the angle-polished probe, the reflected intensity of water is roughly 1% of the backscattered intensity of undiluted Intralipid-20% at 400 nm, the amplitude decreases with the increase of the wavelength to below 0.1% of the backscattered intensity of undiluted Intralipid-20% at 900 nm; for the flat-polished probe, the Fresnel reflection at the fiber-water interface is above 20% of the backscattered intensity of undiluted Intralipid-20%. To correct the residual of the internal reflection in the measurements with the angle-polished probe, when calculating $R_{\angle,\ s}$, $I_{\angle,\ water}$ was subtracted instead of subtracting $I_{\angle,\ \ d}$, since the solvent of undiluted Intralipid-20% and Intralipid-20% dilutions is water. However, the correction for the residual internal reflection when using the angle-polished probe did not improve the accuracy of the measurements dramatically, indicating that although the internal reflection was not completely eliminated, the amplitude was indeed reduced significantly to a level that it does not have a dramatic influence on the results. We do expect that the influence will increase when the refractive index difference between fiber and the solvent of the turbid sample increases. However, it is impossible to correct for the exact residual of the internal reflection for turbid samples with unknown solvents.

The second explanation is that a difference might exist between the collection efficiency of backscattered light of the flat and angle-polished probes. It was assumed that flat- and angle-polished probes made from the fiber of the same batch have an identical light collection efficiency. However, the collection efficiency of the fiber might be different after being polished at 15°. To check whether the collection efficiency changed after polishing, we calculated the reflected intensity ratios of each Intralipid-20% dilution over undiluted Intralipid-20% based on the data obtained using the flat and angle polished probes with Equations (7) and (8).

$$R_{\perp} = \frac{I_{\perp,\text{dilution}} - I_{\perp,\text{water}}}{I_{\perp,\text{IL}} - I_{\perp,\text{water}}} \tag{7}$$

$$R_{\angle} = \frac{I_{\angle,\text{dilution}} - I_{\angle,\text{water}}}{I_{\angle,\text{IL}} - I_{\angle,\text{water}}} \tag{8}$$

The average and SD were calculated for each dilution and plotted in Figure 9. The error bar plotted is one SD. It shows the reflected intensity ratios between Intralipid-20% dilutions and undiluted Intralipid-20% measured by the two probes and clearly indicates that the collection efficiency of the flat and angle polished probe are not identical. The difference between the results obtained using the flat polished probe and the probe polished at 15-degree angle is also wavelength dependent. The more Intralipid-20% is diluted, the larger the difference is, which is due to the fact that the more Intralipid-20% was diluted, the less the diffuse light was collected compared with the amount of large angle scattering light collected (light scattered only a couple of times before being collected by the probe). The large angle scattering light is more sensitive to the exact scattering direction, thus is more sensitive to the collection geometry of the probe.

The difference between the collection efficiency of the flat and angle polished fiber was corrected based on the data shown in Figure 9, and the refractive indices of all Intralipid-20% dilutions were recalculated. The difference between the average of recalculated refractive indices and values from the literature decreased significantly to less than 0.02%. To conclude, the different collection efficiency of the angle-polished probe is the main factor limiting the accuracy of refractive index measurement on turbid media using this technique.

Although the accuracy was significantly improved by applying the correction factor, this approach is only applicable when the refractive index of the solvent is known, which is not feasible for most practical situations where the composition of the sample is unknown.

The average of the measured refractive index of the Intralipid-20% dilution of 1:19 with a glucose concentration of 15 g 100 mL^{-1} is 0.2% higher than the value from literature at 589 nm. The accuracy is lower compared with the accuracy of the measurement on the transparent glucose solution of the same contraction. This difference in accuracy is very likely to be caused by the different collection efficiency of the flat and angle-polished probe similar to the measurements on Intralipid-20% dilutions.

Ding et al [20] measured a higher refractive index of undiluted Intralipid-20% and Intralipid-20% dilutions compared with the measurement results shown in Figure 6. The refractive indices measured by Ding et al. increased with the increase of the lipid concentration. Given the setup used by Ding et al., it was very likely that a weighted value between the refractive indices of water and soybean oil was measured while in our case, the results show that the fiber surface was probably only in contact with water and not with soybean oil particles.

4.3 | In vivo demonstration on the skin

The preliminary demonstration on the skin yielded the refractive index of the skin layer that was in contact with the

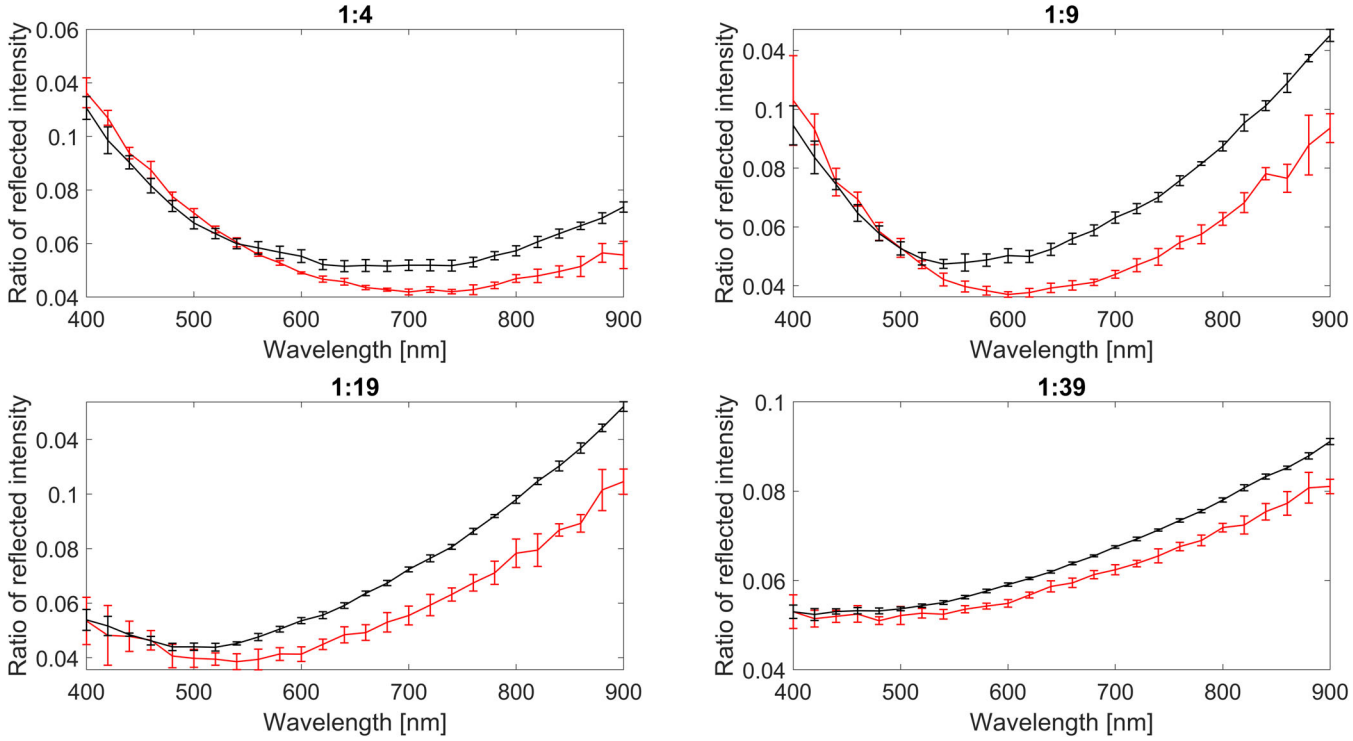

FIGURE 9 Reflected intensity ratios of each Intralipid-20% dilution over undiluted Intralipid-20% (red – flat polished probe; black – angle polished probe)

fiber surface, namely, the stratum corneum layer. The measured refractive indices of the volunteer's skin are in the same range measured previously. [11, 12, 21, 22] To fit the spectral shape of the refractive index spectrum, there are three common models: the Cauchy dispersion equation, the Cornu equation and the Conrady equation. [21] It is easy to verify that none of these models fit the measured refractive indices of the volunteer's skin due to the hemoglobin absorption feature observed between 400 and 700 nm. This type of feature in the refractive index spectrum can originate from several possible sources:

- Strong absorption. Strong absorbing media, such as hemoglobin in red blood cells. The imaginary part of the complex refractive index κ can be obtained from the absorption coefficient μ_a using $\kappa = 4\pi\lambda/\mu_a$. The real part of the complex refractive index can be related to the imaginary part using Kramers Kronig relations. [10] Thus, both the real and imaginary part of the complex refractive index will contain similar hemoglobin spectral features. However, this was not the origin of the hemoglobin absorption feature in Figure 8. During the in vivo demonstration on the skin, the fiber surface was only in contact with the uppermost skin layer, stratum corneum, but not in any contact with any blood.
- Neglecting the imaginary part of the complex refractive index of hemoglobin in the calculation of the Fresnel reflection. When absorption is significant, the imaginary part of the complex refractive index does need to be taken into account in the calculation of the Fresnel reflection. For instance, for hemoglobin solutions of a comparable concentration with red blood cell, the difference in the Fresnel reflection calculated based on the complex refractive index and only the real part of the complex refractive index could be approximately 9% at 436 nm. However, the absorption of the main components of stratum corneum: fat and protein, is minimal in the 400 to 900 nm wavelength range. In this case, the imaginary part of the complex refractive index has negligible influence on the calculation of the Fresnel reflection, Equation (1) holds.
- We believe the hemoglobin absorption feature may be due to non-identical pressure application and optical contact between the measurements done with the flat and angle-polished probes, which were done sequentially. The measurement using the flat-polished probe aimed at collecting the back-scattered light from the skin and the internal reflection due to the refractive index mismatch between fiber and skin, while the measurement using the angle-polished probe aimed at collecting the back-scattered light only. Pressure application will induce tissue composition and structure changes, such as blood volume displacement, interstitial fluid displacement and collagen fiber

density and alignment changes. [23, 24] As a result, the absorption and scattering properties of the tissue will be altered. Different pressure application between the measurements performed with the flat and angle-polished probes will induce changes in tissue optical properties, furthermore, the back-scattered light collected will be different in measured absolute reflectance, which will eventually end up as the bias in the refractive index results. The influence can be seen from the wavy feature in the refractive index spectrum between 400 and 700 nm. However, the pressure application was intended to improve the optical contact between the fiber and skin. The skin surface is not flat and smooth but is laced with multiple networks of fine grooves called sulci cutis. Without pressing the probes onto the skin surface, the fiber surface would be in partial contact with the skin and the other part of the fiber surface will be in contact with water, thus the measured refractive index of the skin would be a weighted average of the refractive index of dry stratum corneum and water.

For measurements on liquid samples, good optical contact with the probe can be easily achieved, while for solid samples, obtaining a good optical contact remains challenging. The accuracy of refractive index measurement with SFR on solid samples depends significantly on the optical contact between the sample and fiber surface. To improve the accuracy of in vivo refractive index measurement with SFR on tissues such as skin, a pressure application control setup is required to reduce the difference in optical contact when performing measurements with the flat and angle-polished probe. Besides pressure application, for elastic samples, surface stretching might be an alternative to the approach to flatten the surface and maximize the contact between fiber and sample.

4.4 | Comparison with existing techniques to measure the refractive index

An overview of the existing instruments to measure the refractive index is shown in Table 1, together with SFR. Most existing techniques are only capable of measuring the refractive index of the sample at a single wavelength because usually a single-wavelength light source is used. To obtain a refractive index spectrum, multiple light sources of the desired wavelengths are required, while a broadband spectrum of refractive index can be obtained when using SFR. The wavelength range depends on the working range of the spectrometer. Furthermore, some instruments require knowledge on the setup. For instance, the refractive index of the refracting prism is required to determine the refractive

TABLE 1 Comparison of refractive index measurement techniques

Method	Broad spectral range with a single measurement	Feasible at NIR-IR range	Assumption/input required	Optical/mechanical alignment needed	Absorbing/turbid media	Contact required	Accuracy (RI value)	Sample status and preparation
Commercial/modified abbe refractometer [7, 8]	No	Possible	Yes: refractive index of the refracting prism	Yes	Yes	Yes	10^{-4}~10^{-5}	Solid and liquid homogenization
OCT [10–12]	No	Yes	No	Yes	Yes	No	10^{-2}	Solid and liquid
White-light interferometry [25]	Yes	Yes	No	Yes	No	No	10^{-3}~10^{-5}	Solid and liquid of known thickness/flatness
Planar reflection [26]	No	Yes	Yes: assumption on NA boundary	Yes	Yes	Yes	10^{-2}~10^{-3}	Solid
Fresnel ratio meter [13]	No	Yes	Measurement fiber core RI	No	Absorbing, but not turbid	Yes	2.5×10^{-5} precision	Solid and liquid
Single fiber reflectance spectroscopy	Yes	Yes	Yes: refractive indices of air and water	No	Yes	Yes	10^{-3}	Solid and liquid

Abbreviations: NIR-IR, near infrared/infrared.

index of the sample when using an Abbe refractometer; the effective index of the fiber is needed to calculate the refractive index of the sample when using a Fresnel ratio meter and so on. This knowledge is not always available for certain setups or is only available at a certain wavelength, while SFR only requires the well-established refractive indices of air and water as an input. Besides, measurements with SFR do not require optical and mechanical alignment compared with most existing techniques. The method can also be applied to absorbing media when the imaginary part of the refractive index is much smaller than the real part of the refractive index. However, when the absorption is significant, the effect of the absorption does need to be taken into account. What's more, sample preparation is required for some of the existing techniques, such as homogenization, while SFR does not require any. Note that two solutions of n_{sample} were found symmetrically around n_{eff} when using SFR. Only the lower value was deemed realistic for our samples in this study. For future application on samples with unknown refractive index, two fibers made from different materials (different effective indices) can be used to manufacture the probes to perform the measurements. Two solutions will be generated for each fiber and one solution should be the same, which is the refractive index of the sample.

5 | CONCLUSION

We developed a method to measure the refractive index for a broad spectrum using SFR. This method can be applied to both transparent and turbid media. For measurement on liquid samples where good optical contact is ensured, the accuracy of the measurement on transparent media is within 0.2%, and the accuracy increases with increasing wavelength. The accuracy of the turbid media is within 0.3% and increases with decreasing wavelength. For measurements on solid samples, the accuracy depends significantly on the optical contact between the fiber and sample surface.

ACKNOWLEDGMENTS

This research was supported by the Netherlands Organization for Scientific Research (Technology Foundation NWO-TTW, iMIT-FIBER Grant No.12702).

AUTHOR BIOGRAPHIES

Please see Supporting Information online.

ORCID

Xu U. Zhang https://orcid.org/0000-0003-1717-7294

REFERENCES

[1] A. L. Post, S. L. Jacques, H. J. C. M. Sterenborg, D. J. Faber, T. G. van Leeuwen, *J. Biomed. Opt.* **2017**, *22*(5), 050501.
[2] A. Wax, V. Backman, *Biomedical Applications of Light Scattering*, McGraw-Hill Education, San Jose, CA **2010**.
[3] J. M. Schmitt, G. Kumar, *Opt. Lett.* **1996**, *21*(16), 1310.
[4] M. L. Dongare, P. B. Buchade, A. D. Shaligram, *Optik (Stuttg)* **2015**, *126*(20), 2383.
[5] K. A. Chang, H. J. Lim, C. B. Su, *Meas. Sci. Technol.* **2002**, *13* (12), 1962.
[6] V. Krishna, C. H. Fan, J. P. Longtin, *Rev. Sci. Instrum.* **2000**, *71* (10), 3864.
[7] G. H. Meeten et al., *Meas. Sci. Technol.* **1991**, *2*(441), 7.
[8] S. Liu, Z. Deng, J. Li, J. Wang, N. Huang, *J. Biomed. Opt.* **2019**, *24*(03), 1.
[9] J. Rheims, J. Köser, T. Wriedt, *Meas. Sci. Technol.* **1997**, *8* (6), 601.
[10] D. J. Faber, M. C. G. Aalders, E. G. Mik, B. A. Hooper, M. J. C. Van Gemert, T. G. Van Leeuwen, *Phys. Rev. Lett.* **2004**, *93*(2), 028102.
[11] G. J. Tearney, M. E. Brezinski, J. F. Southern, B. E. Bouma, M. R. Hee, J. G. Fujimoto, *Opt. Lett.* **1995**, *20*(21), 2258.
[12] A. Knüttel, M. Boehlau-Godau, *J. Biomed. Opt.* **2000**, *5*(1), 83.
[13] C. Kim, C. B. Su, *Meas. Sci. Technol.* **Sep. 2004**, *15*(9), 1683.
[14] S. C. Kanick, H. J. C. M. Sterenborg, A. Amelink, *Opt. Express* **2009**, *17*(2), 860.
[15] Molex, Fiber specification. http://www.literature.molex.com/SQLImages/kelmscott/Molex/PDF_Images/987650-8934.pdf. Accessed 09, 2017.
[16] X. U. Zhang, A. L. Post, D. J. Faber, T. G. van Leeuwen, H. J. C. M. Sterenborg, *J. Biomed. Opt.* **2017**, *22*(10), 1.
[17] E. Sani, A. Dell'Oro, *Opt. Mater. (Amst).* **2016**, *60*, 137.
[18] *CRC Handbook of Chemistry and Physics*, 84th Edition (Ed: D. R. Lide), CRC Press LLC, Boca Ramon, FL **2003**.
[19] M. Daimon, A. Masumura, *Appl. Opt.* **2007**, *46*(18), 3811.
[20] H. Ding, J. Q. Lu, K. M. Jacobs, X.-H. Hu, *J. Opt. Soc. Am. A Opt. Image Sci. Vis.* **2005**, *22*(6), 1151.
[21] H. Ding, J. Q. Lu, W. A. Wooden, P. J. Kragel, X.-H. Hu, *Phys. Med. Biol.* **2006**, *51*(6), 1479.
[22] T. Lister, P. A. Wright, P. H. Chappell, *J. Biomed. Opt.* **2012**, *17* (9), 0909011.
[23] R. Reif, M. S. Amorosino, K. W. Calabro, O. A'Amar, S. K. Singh, I. J. Bigio, *J. Biomed. Opt.* **2008**, *13*(1), 010502.
[24] S. A. Carp, T. Kauffman, Q. Fang, E. Rafferty, R. Moore, D. Kopans, D. Boas, *J. Biomed. Opt.* **2006**, *11*(6), 064016.
[25] D. Mazzoni, M. Galli, F. Marabelli, *IEEE J. Quantum Electron.* **1982**, *18*(10), 1509.
[26] F. P. Bolin, L. E. Preuss, R. C. Taylor, R. J. Ference, *Appl. Opt.* **1989**, *28*(12), 2297.

How to cite this article: Zhang XU, Faber DJ, Post AL, van Leeuwen TG, Sterenborg HJCM. Refractive index measurement using single fiber reflectance spectroscopy. *J. Biophotonics*. 2019;12: e201900019. https://doi.org/10.1002/jbio.201900019